Universität Freiburg
Advanced Physics Lab Course
FP1 2024-2

Experiment 8
Semiconductors

Short Report

[redacted]

August 27, 2024

Lab Work conducted: August 23 & 26

Assistant: [redacted]

Contents

1 Objectives **2**

2 Equipment used **2**

3 Procedure **2**

3.1 Procedure Part 1: Energy Bandgap E_g 3

3.2 Procedure Part 2: Semiconductor Detector 4

4 Observations, Data and Analysis **5**

4.1 Analysis Part 1: Energy Bandgap E_g 5

4.1.1 General Analysis Procedure 5

4.1.2 Silicon 7

4.1.3 Germanium 9

4.2 Analysis Part 2: Semiconductor Detector 11

4.2.1 Spectra recorded with the Si-detector 12

4.2.2 Spectra recorded with the CdTe detector 14

4.2.3 Comparing the two detectors 15

5 Discussion **16**

5.1 Discussion Part 1: Energy Bandgap E_g 16

5.2 Discussion Part 2: Semiconductor Detector 17

6 Improvements and Suggestions **18**

7 Conclusion **19**

8 Appendix A: Calculation for energy calibration **20**

9 Appendix B: Additional Plots **21**

10 Appendix C: Signed Lab Notes **22**

1 Objectives

This series of experiments is dedicated to learning about some basic properties and applications of semiconductors and consists of two different parts. In the first part, the bandgap energy E_g of the two semiconductors Si and Ge will be determined using optical grating spectroscopy and measuring the transmission and absorption spectra.
In the second part, detector systems using a pure semiconductor diode (Si) and a compound semiconductor ohmic contact (CdTe-Au) respectively will be used to record the spectra of two radioactive isotopes (^{57}Co & ^{241}Am) and estimate the relative absorption probabilities $Abs_{\mathrm{Si}}/Abs_{\mathrm{CdTe}}(E)$ as well as the relative energy resolution $RER(E)$ at three different energies E for both detectors as measures of detector quality.

2 Equipment used

For the first experiment, with a setup as shown in fig. 1, we used a spectrometer with an optical grating placed on a rotating platform. In detail, this spectrometer consists of a lamp, a chopper periodically cutting the light into short pulses, a lens to collimate the light into parallel rays falling onto the grating, a second collimation lens, a filter (to filter out higher order interference) and a pyrodetector, in front of which the semiconductor sample is placed.

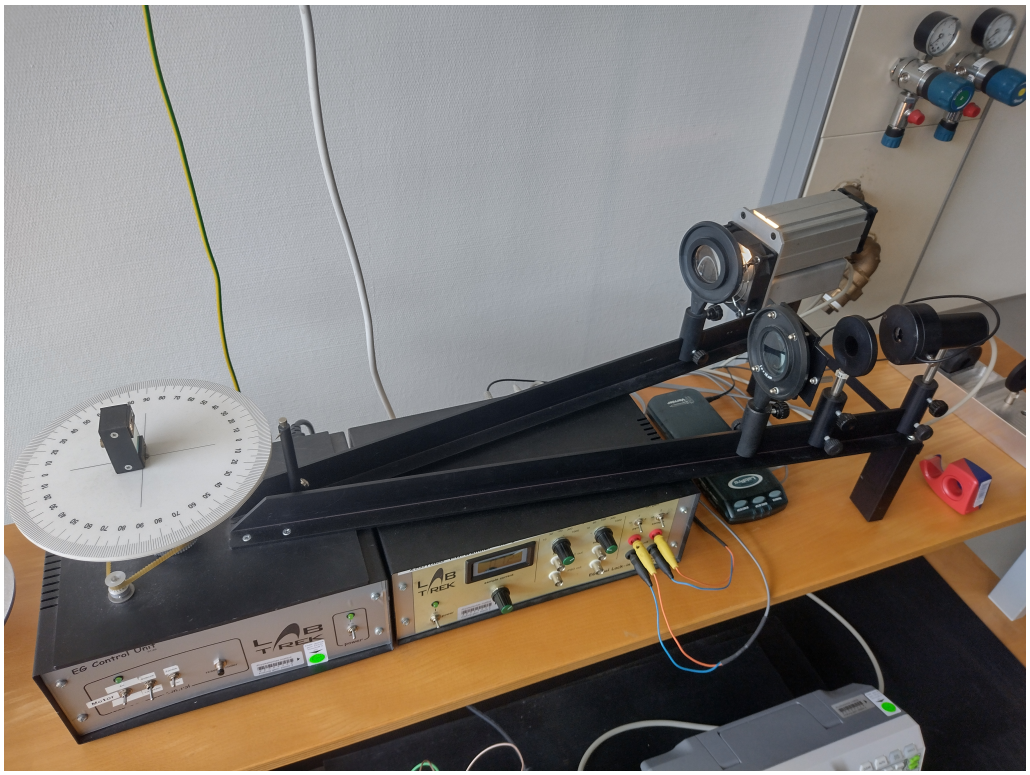

Figure 1: Setup for the band gap measurements

For the second experiment, a detector system already pre-assembled in a detector box was used (see fig. 2). This system consisted of the detector itself (Si-diode or CdTe-crystal with ohmic contact to Au respectively) on a small board, a pre-amplifier and a shaping amplifier. The detector box was then connected to an ADCMCA, which was in turn connected to a computer with the data acquisition software *ADMCA*. More technical details are omitted in this short report for the sake of keeping it brief, but can be found in either the lab instructions [Fre] or the underlying thesis [Amr08].

3 Procedure

It should be noted, that the experiments were not conducted in the order they are listed in this report. Due to the low activity of especially the ^{57}Co sample, long data taking times were required

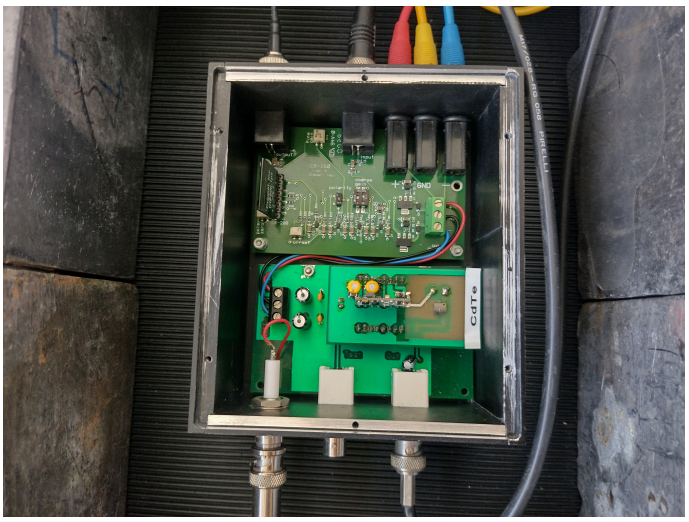

Figure 2: Detector system for part 2 of the experiment

in order to obtain reasonable spectra. The measurements for part two were thus run in the background whilst other experiment was conducted.

3.1 Procedure Part 1: Energy Bandgap E_g

For the first experiment, the setup in fig. 1 was used. We describe the different relevant angles in the experiment as illustrated in fig. 3

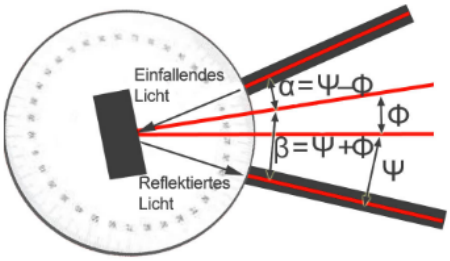

Figure 3: Angles used in the description of part 1. This picture is taken from Amr08. Ψ is fixed in the experiment and is known to be 7.5°.

First, the Germanium semiconductor probe on its circular holder was placed directly in front of the pyrodetector and the correctly labelled grating on a rotating platform was mounted on its post opposite to the lamp and the sample. The grating used for Ge had a spacing of $g_{\mathrm{Ge}} = 600\,\frac{\mathrm{lines}}{\mathrm{mm}}$ (Fre). The correct filter was chosen as well and placed between the lens and the probe on the second arm of the spectrometer. Before any measurements were taken, the beam path was slightly optimised in terms of modifying the width of the aperture and the positions of the lenses, in order to ensure that the light beam would follow the two spectrometer arms nicely and parallel. In the optimised setup, the width d of the aperture was approximately

$$d \approx 2\,\mathrm{cm}$$

and the distance x between the optical grating (at $\Phi = 0°$) and the lens on the second arm as measured with a measuring tape

$$L \approx 56\,\mathrm{cm}.$$

The width of the optical gratings is

$$D \approx 2.5\,\mathrm{cm}.$$

These values will be used later in order to estimate a systematic error on the end result, stemming from the energy resolution of the spectrometer.
Next, the lamp and electronics were turned on. The wiring was already preinstalled, but the U-I-converter current had to be set to $\approx 15\,\mathrm{mA}$, as suggested in the lab instructions. The optical grating was manually turned to $\Phi = 0$ and the analysis software *LoggerPro* was started. In the software, the chosen zero point was set by pressing the corresponding button. A program with settings specific to the investigated probe could be loaded into the software. Some test measurements were run in order to find gain settings for both the pyro (transmission) and the sample (absorption) channels with which the 1st order interference maxima would not reach the cut-off limit of 5 V. The gain settings chosen for Ge were 1000 (maximum gain achievable) for both channels.

Thereafter, four different measurements were taken. The first one was a measurement of both the transmission and the absorption spectrum. For the second measurement, the sample was covered tightly with a thick leather wallet and the spectra of both the backgrounds of transmission and absorption were recorded. During those two measurements and the last one, during which the probe was removed in order to obtain the radiation power of the lamp through the lenses and filters, the turntable was rotated slowly from approximately -90° to +90°. The third measurement was designed to get a handle on the uncertainty of the spectra. Therefore, 50 values were recorded at a constant angle ($\approx 37\,^\circ$ for Ge and ≈ 42 $for Si$). $The angle was chosen to lie close to the 1. order transmission and absorption max$
$After the measurements with Ge were completed, the Si probe was placed in front of the pyro detector and the optical grating$
$1200\frac{\mathrm{lines}}{\mathrm{mm}}$ and the U-I-converter current had to be set to $\approx 0.75\,\mathrm{mA}$ (see [Fre]). For this probe, the chosen gain settings were 1000 for the pyro channel and 10 for the sample channel. All distances could be kept the same and after a new $\Phi = 0$ position had been set, the same four measurements as for the Ge probe were conducted. For the measurement of the lamp´s radiation power, the pyro gain had to be reduced to 100, in order to avoid a cut-off.

3.2 Procedure Part 2: Semiconductor Detector

For the first half of this part the Si diode was used. Initially, the ^{57}Co sample was placed on top of the detector box. The data acquisition software was started and the preset live time and threshold set. The chosen settings for all measurements in this part are summarised in table 1. We kept varying the threshold in-between the measurements, trying to find the most suitable value. After the spectrum with ^{57}Co was taken, the radioactive probe was switched for the ^{241}Am sample.

detector	isotope	preset live time [h]	threshold
Si-diode	^{57}Co	3	100
Si-diode	^{241}Am	1	75
CdTe-crystal	^{57}Co	1	50
CdTe-crystal	^{241}Am	1	25

Table 1: Settings for the spectra acquisition in Part 3

The measurements with the CdTe-crystal had to be performed on the second lab day, but were conducted accordingly. Since the data acquisition software kept crashing on day 2 and multiple long measurements have been lost, we only took a 1 h instead of a 3 h measurement with the CdTe detector and the ^{57}Co sample.

4 Observations, Data and Analysis

4.1 Analysis Part 1: Energy Bandgap E_g

4.1.1 General Analysis Procedure

In this part of the experiment, we determined the transmission rate (measured by the pyrodetector) and the absorption rate (detected through the current flowing through the semiconductor sample) as a function of the angle Φ (indicated in fig. 3) at which the grating was positioned at a given time. From simple geometric considerations and using the well-known Planck-Einstein relation $E = h\,\nu$, where h is the Planck constant and ν the frequency, one can get the relationship between the angle Φ and the energy E of the photons hitting the sample in the 1st order maximum of the spectrometer's interference pattern [Fre]:

$$E(\Phi) = \frac{h\,c}{2\,g^{-1}\,\cos(\Psi)\,\sin(\Phi)}, \tag{1}$$

wherein g^{-1} is the lattice constant of the optical grating used and $\Psi = 7.5$ half of the angle between the two spectrometer arms.

The spectra obtained were loaded into Python for further analysis. Here follows first a general description of how the data analysis for this part was done and the actual results and plots for the two different probes, Si and Ge, are then shown in section 4.1.2 and section 4.1.3 respectively.

In order to obtain uncertainties on the absorption and transmission spectra, the third measurement (compare section 3.1) was used. From the N values x_i taken at a constant angle, the empirical standard deviation

$$\sigma = \sqrt{\frac{1}{N-1}\sum(x_\mathrm{i} - \bar{x})^2}$$

was calculated. This statistical uncertainty was then assumed to be approximately the same for all data points in the respective spectrum and can be seen as errorbars in figs. 6 to 9. It was assumed that the uncertainties on the background and lamp spectra are negligible for the further calculations.

In a next step, the absorption and transmission spectra were corrected for the background radiation and normalised with respect to the spectrum of the lamp and filter:

$$Trans_\mathrm{real} = \frac{Trans - Background_\mathrm{trans}}{Lamp}$$
$$Abs_\mathrm{real} = \frac{Abs - Background_\mathrm{abs}}{Lamp}.$$

The hereby obtained corrected spectra $Trans_\mathrm{real}(E)$ and $Abs_\mathrm{real}(E)$ were plotted in the same graph.

The bandgap energy E_g is the energy at which the transmission of light is reduced and the absorption of light into the semiconductor sample shows an increase, when moving in the direction from lower to higher photon energies. Such a crossover of the transmission and absorption spectra could indeed be observed for both of the 1st order interference maxima. For the region around both of those maxima, the following procedure was then carried out, following the instructions manual [*Fre*]:

1. The steeply rising part of the absorption spectrum as well as the steeply falling part of the transmission spectrum were fit with a straight line.
2. These straights were then intersected with horizontal lines through the absorption minimum and the transmission maximum at lower energies than the crossing.
3. From the intersection points two values for E_g were obtained. The arithmetic mean of those two values was taken to get a first estimation of E_g.

In this last step, the standard deviation on the mean functions as an estimator of the uncertainty.

Throughout the experiment, the "$\Phi = 0$"- position of the optical grating was chosen manually and by eye. There were several instances at which this had to be readjusted during the experiment, as the data acquisition software seemed to keep loosing the set point for some unknown reason. It seems reasonable to assume that a systematic error might have occurred due to this manual alignment. This systematic error can however be cancelled out, by taking the average of the results of above described procedures for both the right and the left maximum.

A second systematic uncertainty we tried to take into account is the following: as the optical grating and the aperture both have a certain width, there is never exactly one photon energy E falling onto the sample at a given angle Φ. In this paragraph, we want to estimate the systematic error on the photon energy resulting from said energy resolution of the spectrometer, closely following the calculations and explanation found in chapter 3.4 of [Amr08] and using the same names for the involved factors.

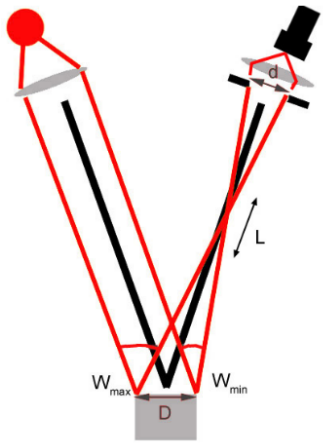

Figure 4: Sketch for estimation of energy resolution of the spectrometer. Taken from [Amr08].

For simplicity, we neglect the uncertainties on the quantities d, L and D, the measured values of which can be found in section 3.1. Additionally, we only do the following calculation of the systematic error on the photon energy for the best value of the band gap E_g, and not for the entire spectrum.
From geometrical considerations it follows that the maximum and minimum angles $W_{\min}$ and $W_{\max}$ under which light coming from the grating still reaches the probe at a certain angle Φ are given as

$$W_{\min} = \Psi + \arcsin\left(\frac{\sin(\Psi)\, L - D/2\, \cos(\Phi) - d/2\, \cos(\Psi)}{L}\right)$$
$$W_{\max} = \Psi + \arcsin\left(\frac{\sin(\Psi)\, L + D/2\, \cos(\Phi) + d/2\, \cos(\Psi)}{L}\right),$$

resulting in a systematic uncertainty

$$s_{\mathrm{E}} = \frac{1}{2}\left(\frac{h\,c}{2\,g^{-1}\,\cos(\Psi)\,\sin(W_{\min}/2)} - \frac{h\,c}{2\,g^{-1}\,\cos(\Psi)\,\sin(W_{\max}/2)}\right).$$

Finally, we quadratically add up the above discussed systematic uncertainty s_{E} and the uncertainty stemming from the fit s_{fit} in order to obtain a total uncertainty on our best value for E_g:

$$s_{Eg} = \sqrt{s_{\mathrm{E}}^2 + s_{\mathrm{fit}}^2}$$

4.1.2 Silicon

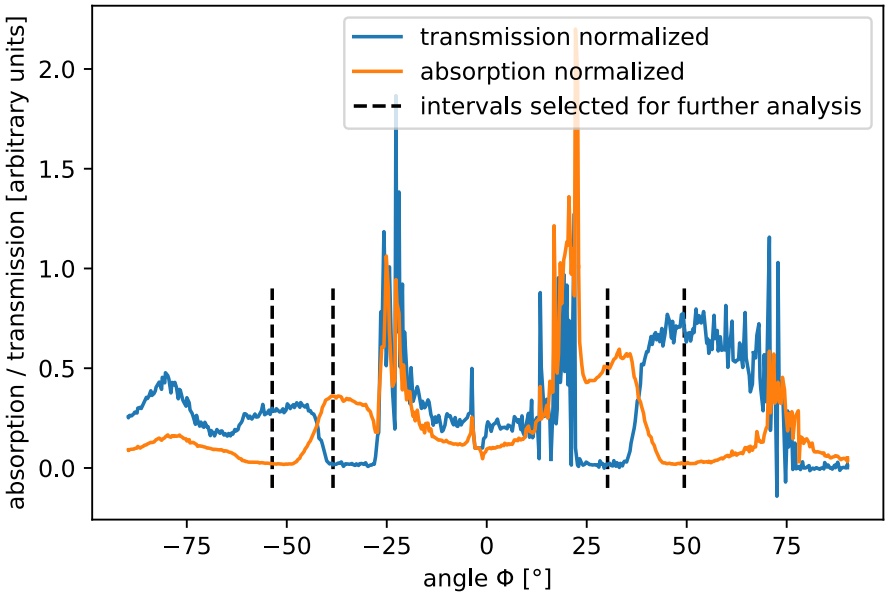

Figure 5: Normalised and corrected absorption and transmission spectra for Si as a function of the angle Φ. The areas on which the further analysis is done are highlighted.

A plot with the normalised and background-corrected transmission and absorption spectra for the silicon sample can be found in fig. 5. A figure with the uncorrected spectra is attached as fig. 17 in Appendix B. It is noticeable that the errorbars on the transmission spectrum are much larger than the ones on the absorption spectrum. This shows that the pyrodetector seems to cause a larger statistical fluctuation than the absorption measured directly through the current flowing trough the sample. In fig. 5 two areas are marked by dashed lines. These are the angle regions of interest, where the transmission and absorption curves cross over.

To these two regions, the fitting procedure described in section 4.1.1 was applied. The results of these fits are illustrated in fig. 6 and fig. 7 respectively.

The black vertical lines in the two plots indicate the intersection points of the linear fits with the horizontal lines. On the first side, the arithmetic mean of the two intersection points is:

$$E_{\mathrm{Si},1} = 1.108(9)\,\mathrm{eV}$$

and on the second side:

$$E_{\mathrm{Si},2} = 1.04(2)\,\mathrm{eV}$$

where the uncertainty on those values is given by the standard deviation of the mean.

In order to correct for a potential systematic error in the choice of the zero-degree point, the arithmetic mean between the two results is calculated:

$$E_{\mathrm{Si,mean}} = 1.07(2)\,\mathrm{eV},$$

where $s_{\mathrm{fit}} = 0.02\,\mathrm{eV}$ is the total statistical uncertainty through the fitting process.

Additionally, the systematic uncertainty stemming from the energy resolution of the spectrometer is calculated as described in section 4.1.1:

$$W_{\mathrm{min,\ Si}} = 13$$
$$W_{\mathrm{max,\ Si}} = 17$$
$$s_{\mathrm{E,\ Si}} = 0.4\,\mathrm{eV}$$

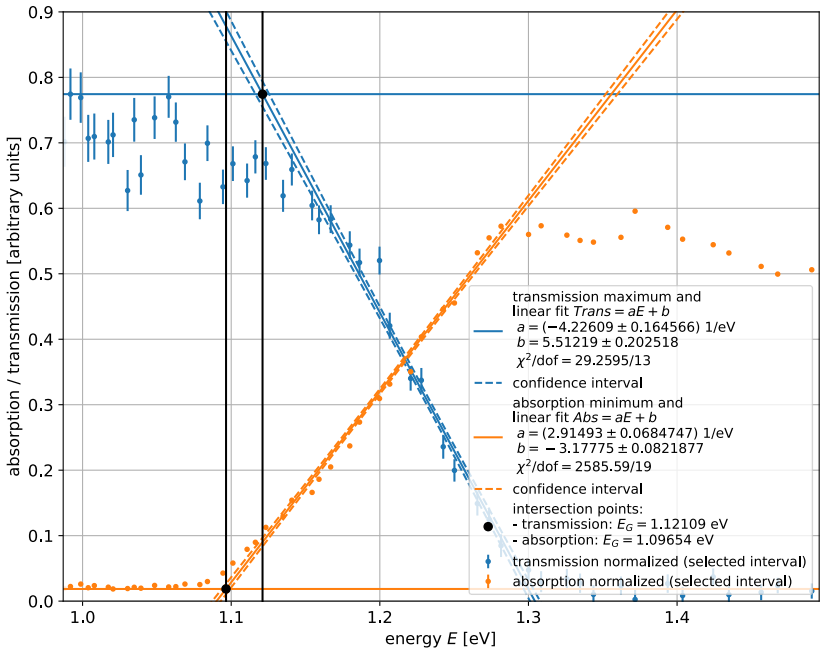

Figure 6: Fit on first side for the Si transmission and absorption spectra. Here the spectra are shown as a function of photon energy E. The optimal fit values and their uncertainties are given in the legend.

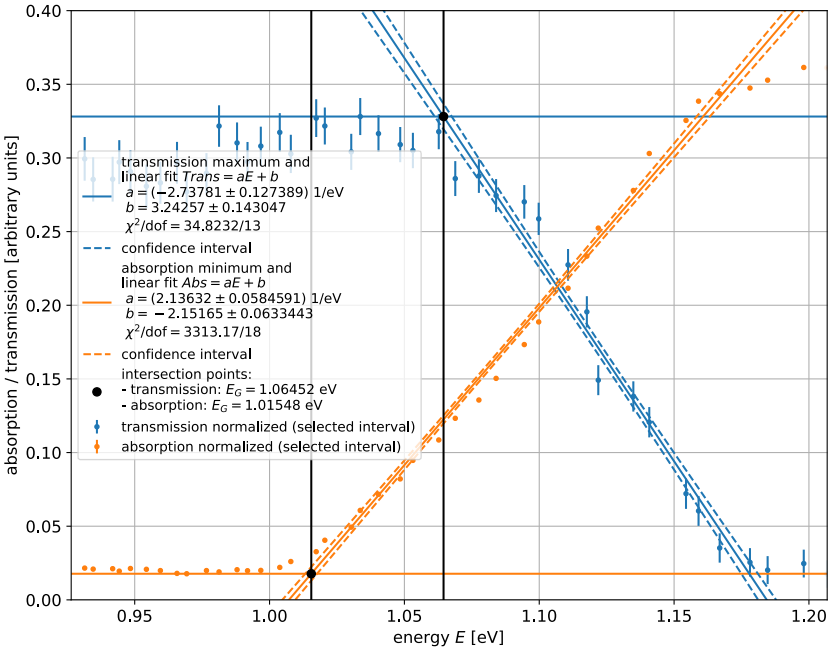

Figure 7: Fit on second side for the Si transmission and absorption spectra. Here the spectra are shown as a function of photon energy E. The optimal fit values and their uncertainties are given in the legend.

One can see that this is a much higher uncertainty than the one stemming from the statistical evaluation of the fits. We add the uncertainties quadratically to get the total uncertainty:

$$s_{\mathrm{g,Si}} = \sqrt{s_{\mathrm{fit,Si}}^2 + s_{\mathrm{E,Si}}^2} \approx 0.42$$

The final result for the bandgap of Si is thus:

$$E_{\mathrm{g,\ Si}} = 1.07(42)\,\mathrm{eV} \tag{2}$$

4.1.3 Germanium

For the Germanium sample, the same evaluation steps were carried out as for the Silicon sample.

It is striking, however, that the normalised and corrected spectra for Germanium look somehow much messier than the ones for Silicon and one has to zoom in quite a bit in order to clearly see the areas where the transmission and absorption trends intersect. Besides, the errorbars on especially the transmission spectrum are much larger than the ones for Silicon and also vary more in size.

A plot with the uncorrected data of the transmission and absorption spectra and the marked relevant intervals for the further analysis can be found in fig. 18 in appendix B. The fits on the relevant regions left and right from the centre are illustrated in fig. 8 and fig. 9.

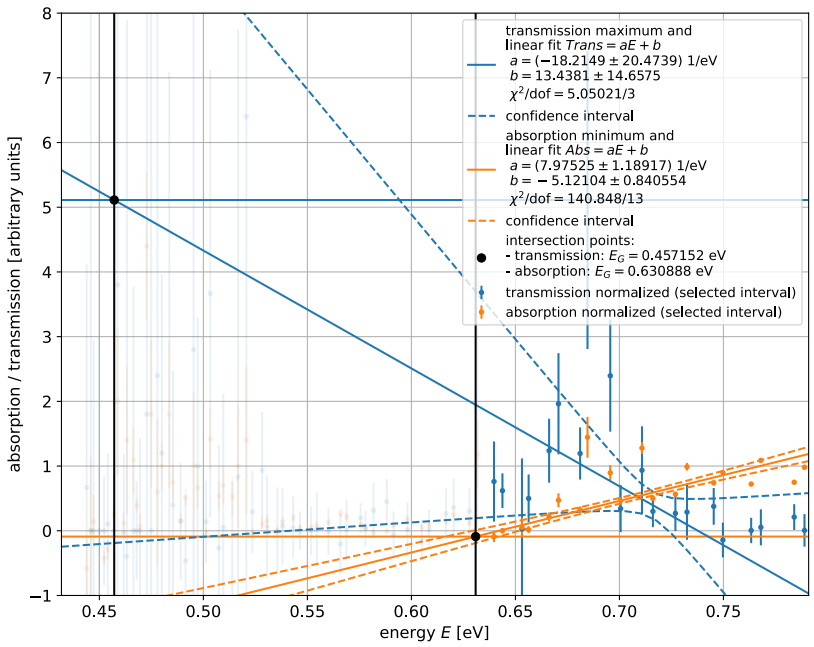

Figure 8: Fit on first side for the Ge transmission and absorption spectra. Here the spectra are shown as a function of photon energy E. The optimal fit values and their uncertainties are given in the legend.

Again, we use the intersection points on both sides and calculate the means between the upper and the lower intersection point:

$$E_{\mathrm{Ge},1} = 0.54(6)\,\mathrm{eV}$$
$$E_{\mathrm{Ge},2} = 0.58(4)\,\mathrm{eV}$$

The mean between those two values is given by

$$E_{\mathrm{Ge,mean}} = 0.563(94)\,\mathrm{eV}$$

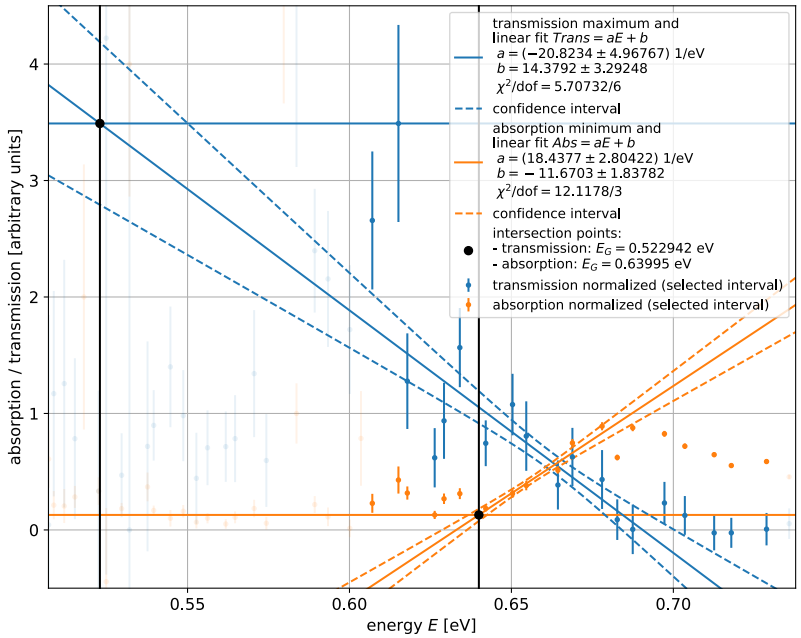

Figure 9: Fit on second side for the Ge transmission and absorption spectra. Here the spectra are shown as a function of photon energy E. The optimal fit values and their uncertainties are given in the legend.

The systematic error due to the energy resolution of the spectrometer was also in this case larger than the uncertainty from the fit:

$$\begin{aligned} W_{\text{min, Ge}} &= 13 \\ W_{\text{max, Ge}} &= 17 \\ s_{\text{E, Ge}} &= 0.37\,\text{eV} \end{aligned}$$

leading to a total uncertainty of

$$s_{\text{g, Ge}} \approx 0.38$$

The final result for the bandgap of Ge thus is

$$E_{\text{g,Ge}} = 0.56(38)\,\text{eV} \tag{3}$$

4.2 Analysis Part 2: Semiconductor Detector

The objective of this experiment is to compare and quantify the suitability of two different semiconductor detectors with each other. The radioactive sources of ^{57}Co and ^{241}Am have known most probable decays, which makes it possible to later do an energy calibration. The decay schemes with the most probable decays are illustrated in fig. 10.

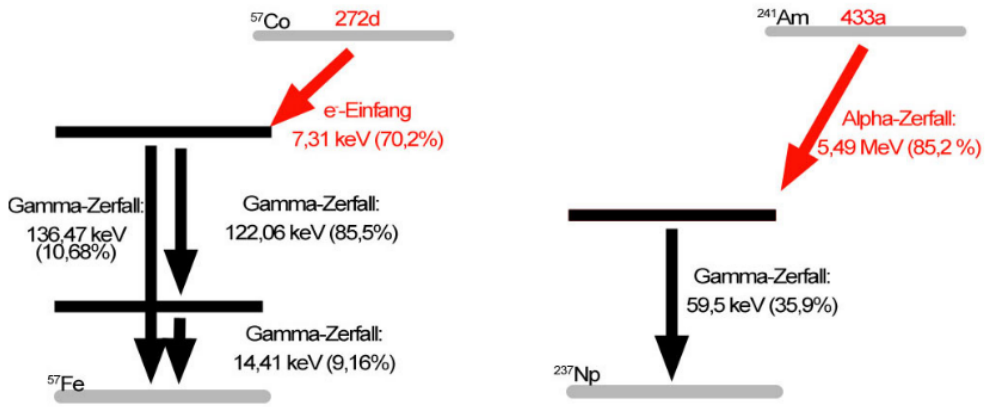

(a) Zerfall von ^{57}Co (b) Zerfall von ^{241}Am

Figure 10: Relevant decays of the isotopes used in part 3 of this experiment. This image is taken from [Amr08].

The spectra recorded in the data acquisition software *ADMCA* all feature a larger photopeak towards the left of the acquisition window and a drawn out background towards the right. The Compton continuum that one might expect to see in a typical gamma spectrum is cut off in some of the measurements by the threshold, as it would be located at lower channel numbers in comparison to the big photopeak. A photopeak occurs when a gamma ray deposits all of its energy in the detector medium.
From the decay schemes (fig. 10), one would expect the biggest peaks to appear at 122.06 keV and 136.47 keV (smaller) for ^{57}Co and at 59.5 keV for ^{241}Am.

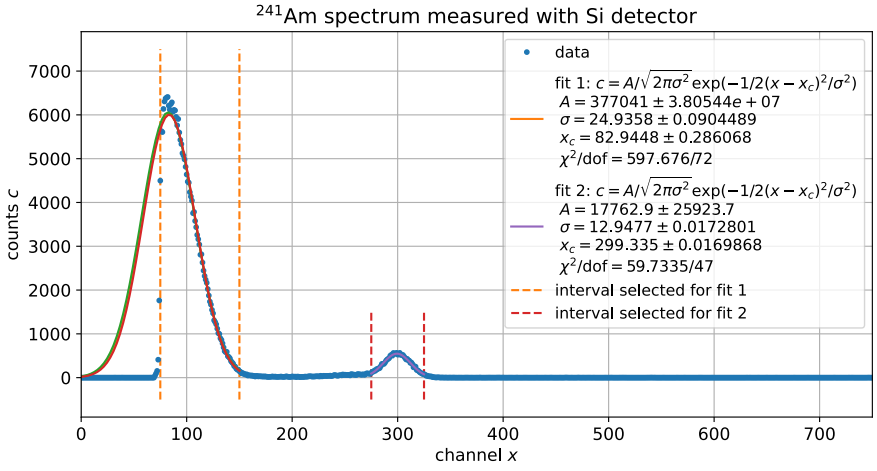

Figure 11: ^{241}Am spectrum recorded with the Si detector with Gaussian fits to the visible peaks

A first qualitative observation one can make when recording the spectra (figs. 11 and 12) is the fact that the ^{57}Co sample seems to have a much lower activity than the ^{241}Am sample, as the rate of recorded events is much lower. This was already taken into account when choosing the data acquisition time for ^{57}Co to be much longer. Besides, the spectrum of cobalt looks much less clean and there is much more noise.

For further analysis, the spectra are loaded into python. We assume a Poisson error on the number

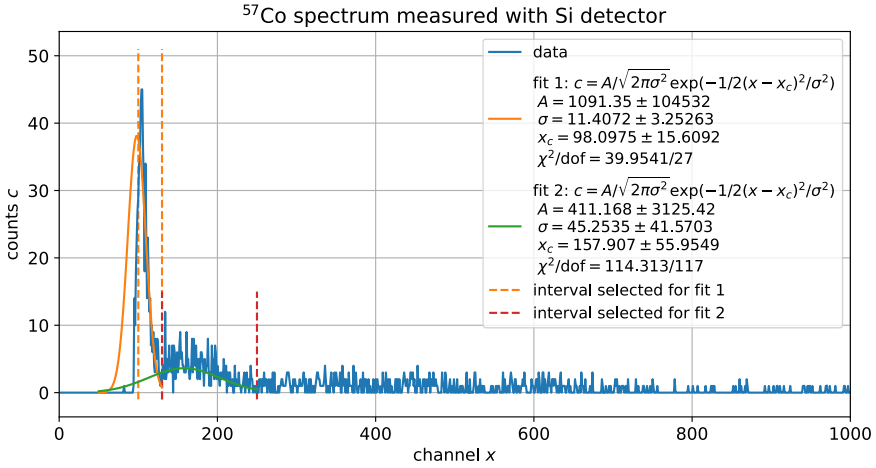

Figure 12: ^{57}Co spectrum recorded with the Si detector with Gaussian fits to the visible peaks

of counts in each channel (or, respectively, an error of one count for the channels with zero counts). This error is later taken into account for fits.

4.2.1 Spectra recorded with the Si-detector

In the ^{57}Co-spectrum recorded with the Si detector, there is an obvious peak around channel 100, which we interpret to be the expected 122.06 keV photopeak, but the second peak (expected at 136.47 keV) is barely discernible. In the case of ^{241}Am, there are unexpectedly not one, but two clear peaks. The bigger photopeak must be the expected one at 59.9 keV. But when looking at the decay scheme, one would not expect another well visible peak to appear at higher energies/channel numbers than the biggest peak. This is why we expect the second peak in the ^{241}Am spectrum to either be part of the background spectrum (which is unlikely as it is not visible in the ^{57}Co spectrum) or stem from a different isotope altogether. This could for example be the dopant of the Si detector.

For the sake of keeping the experimental expenditure lower, no background measurement was taken in this experiment. This can also be justified by the fact that we are mostly interested in relative values (e.g. relative absorption probabilities) between the two investigated detectors, where the background would partially cancel out anyways.

After having already taken the spectrum for ^{57}Co, it occurred to us that the threshold might have been chosen a bit to high, as the photopeak seems to be cut off partially on the left side. This was taken into consideration during the following measurements by choosing a higher threshold setting.

All the chosen photopeaks are fitted with Gaussian curves of the shape

$$c(x) = A\,\frac{1}{\sqrt{2\,\pi\sigma^2}}\,\exp\left(-\frac{(x-x_\mathrm{c})^2}{2\,\sigma^2}\right),$$

where $c(x)$ denotes the number of counts in channel x, A related to the amplitude of the peak, x_c the channel around which the peak is centred and σ the width of the peak. The results of those fits can be seen in fig. 11 and fig. 12, where the optimal fit parameters are given in the legends.

An energy calibration can be done by assigning the centre channel values x_c to the known photopeak energies. Then a linear fit of the form

$$E(x_\mathrm{c}) = a\,x_\mathrm{c} + b$$

can be performed in order to obtain the desired relationship. The energy values used for the expected photopeaks are: 59.9 keV for ^{241}Am, as well as 122.06 keV and 136.47 keV for ^{57}Co. The resulting linear fit is illustrated in fig. 13.

The channel-energy relationship for the Si detector is thus given by:

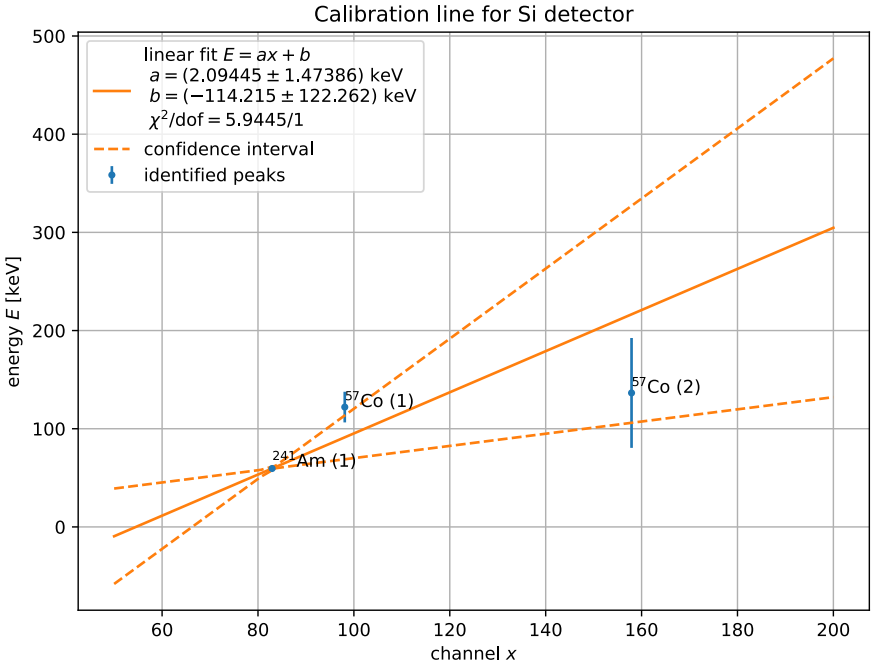

Figure 13: Energy calibration for the Si detector: linear fit to three known photopeaks.

$$E_{\mathrm{Si}}(x_{\mathrm{c}}) = 2.09 \cdot x_{\mathrm{c}} - 114.22\,\mathrm{keV}$$

In order to convert the amplitude A and the width σ of the fitted peaks into the energy scale, we use the conversion calculations and error propagations derived in detail in section 8 (Appendix A). This gives us for the spectra recorded with the Si detector:

$$A_{\mathrm{Si}}(59.9\,keV) = 0.79(7.97) \cdot 10^6\,\mathrm{keV} \tag{4}$$
$$\sigma_{\mathrm{Si}}(59.9\,keV) = 52(37)\,\mathrm{keV} \tag{5}$$
$$A_{\mathrm{Si}}(122.06\,keV) = 0.023(2.2) \cdot 10^5\,\mathrm{keV} \tag{6}$$
$$\sigma_{\mathrm{Si}}(122.06\,keV) = 24(18)\,\mathrm{keV} \tag{7}$$
$$A_{\mathrm{Si}}(136.47\,keV) = 0.86(6.58) \cdot 10^3\,\mathrm{keV} \tag{8}$$
$$\sigma_{\mathrm{Si}}(136.7\,keV) = 95(109)\,\mathrm{keV} \tag{9}$$

4.2.2 Spectra recorded with the CdTe detector

For the spectra recorded with the CdTe crystal detector, the same fitting procedure is applied. At first glance, the ^{241}Am spectrum does not look very different in terms of resolution or noise from the one recorded with the Si detector. The ^{57}Co spectrum looks noisier than before, which is due to the lower data acquisition time. The form of the spectra, however, is clearly different since we have used lower thresholds here, so that a larger range of the spectrum is visible.

In the ^{241}Am spectrum (see fig. 14), we observe very large rates directly at the threshold that we assume to be noise. Cutting that off, we recognise a clear photopeak around channel 300 and, to the left of it, a Compton continuum with additional peaks that are probably produced by fluorescence effects or by electron escapes after pair production. The smaller second peak that we observed with the Si detector to the right of the large photopeak is not visible here, which again supports the theory that it was connected to the Si detector material and not e.g. the background.

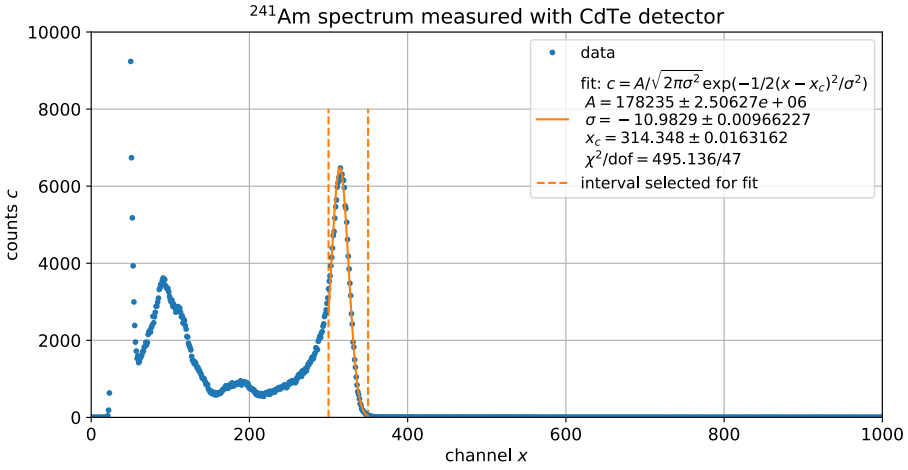

Figure 14: ^{241}Am spectrum recorded with the CdTe detector with a Gaussian fit to the visible photopeak

On the second lab day, during which the measurements with the CdTe detector were taken, a reoccurring problem with the data acquisition software, which kept crashing and loosing all so far recorded data, lead till the fact that the procedure for the measurement of the ^{57}Co spectrum had to be adjusted. Instead of taking a three hour long measurement as with the Si detector, it was in the end unfortunately only possible to obtain a 1 h measurement. In order to make the data comparable to the ^{57}Co spectrum obtained with the Si detector, the whole set was scaled up by a factor of three. The uncertainty on the number of counts in each bin was scaled up accordingly, which is why the errorbars appear so huge in fig. 15. The spectrum is in addition very noisy. A bigger photopeak as well as what might be the second smaller expected peak to its right are fitted and used to perform an energy calibration for the CdTe detector.

The energy calibration is in this case given by:

$$E_{\mathrm{CdTe}}(x_c) = 0.195 \cdot x_c - 1.7 \tag{10}$$

Using the channel-to-energy conversion, the amplitudes and widths of the fitted peaks are given by:

$$A_{\mathrm{CdTe}}(59.9\,keV) = 34677(487612)\,\mathrm{keV} \tag{11}$$
$$\sigma_{\mathrm{CdTe}}(59.9\,keV) = 2.137(034)\,\mathrm{keV} \tag{12}$$
$$A_{\mathrm{CdTe}}(122.06\,keV) = 325(2272)\,\mathrm{keV} \tag{13}$$
$$\sigma_{\mathrm{CdTe}}(122.06\,keV) = 5(1)\,\mathrm{keV} \tag{14}$$
$$A_{\mathrm{CdTe}}(136.47\,keV) = 6.7(30.5)\,\mathrm{keV} \tag{15}$$
$$\sigma_{\mathrm{CdTe}}(136.7\,keV) = 0.96(1.04)\,\mathrm{keV} \tag{16}$$

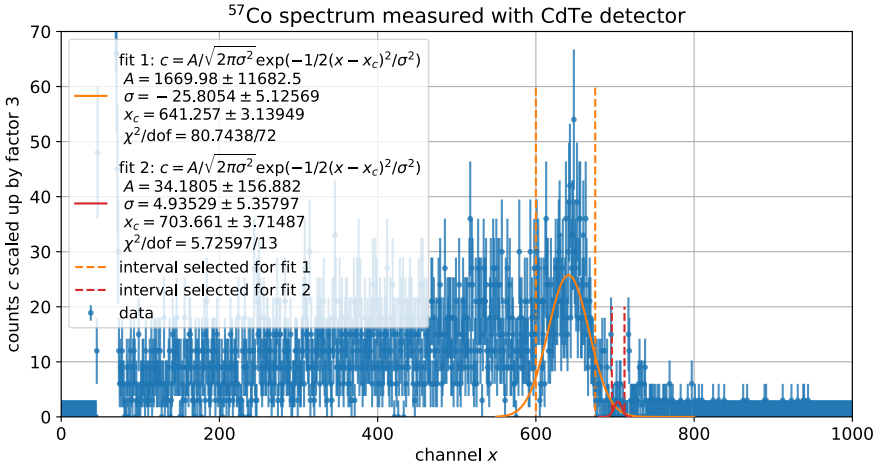

Figure 15: ^{57}Co spectrum recorded with the CdTe detector with Gaussian fits to the visible photopeaks

4.2.3 Comparing the two detectors

One way of comparing the performance of the two detector systems is to take a look at the relative absorption probabilities at different energies. The absorption probability $Abs(E)$ at a certain energy E can be calculated as the ratio between the amplitude A of the photopeak and a detector specific constant called the active area a:

$$\frac{Abs_{\mathrm{Si}}}{Abs_{\mathrm{CdTe}}}(E) = \frac{A_{\mathrm{Si}}/a_{\mathrm{Si}}}{A_{\mathrm{CdTe}}/a_{\mathrm{CdTe}}}. \tag{17}$$

The values for the active areas are given in the lab instructions [Fre] as

$$a_{\mathrm{Si}} = 100\,\mathrm{mm}^2$$
$$a_{\mathrm{CdTe}} = 23\,\mathrm{mm}^2$$

The uncertainties are propagated according to Gaussian error propagation, and assuming the uncertainties on the active areas to be negligible:

$$s_{\mathrm{Abs,si\ /\ Abs,CdTe}} = \sqrt{\left(\frac{a_{\mathrm{CdTe}}}{A_{\mathrm{CdTe}}\,a_{\mathrm{Si}}}\,\Delta A_{\mathrm{Si}}\right)^2 + \left(\frac{A_{\mathrm{Si}}\,a_{\mathrm{CdTe}}}{a_{\mathrm{Si}}\,A_{\mathrm{CdTe}}^2}\,\Delta A_{\mathrm{CdTe}}\right)^2}$$

With this we obtain the following results for the different peaks:

$$\frac{Abs_{\mathrm{Si}}}{Abs_{\mathrm{CdTe}}}(59.9\,\mathrm{keV}) = 5(534) \tag{18}$$
$$\frac{Abs_{\mathrm{Si}}}{Abs_{\mathrm{CdTe}}}(122.06\,\mathrm{keV}) = 2(155) \tag{19}$$
$$\frac{Abs_{\mathrm{Si}}}{Abs_{\mathrm{CdTe}}}(136.47\,\mathrm{keV}) = 30(265) \tag{20}$$

Finally, the two detectors should be compared in terms of their relative energy resolution RER in the photopeaks, which is defined as

$$RER(E) = \frac{FWHM}{E} = \frac{2\sqrt{2\,\ln(2)}\,\sigma}{E} \tag{21}$$

with a corresponding uncertainty that is given by

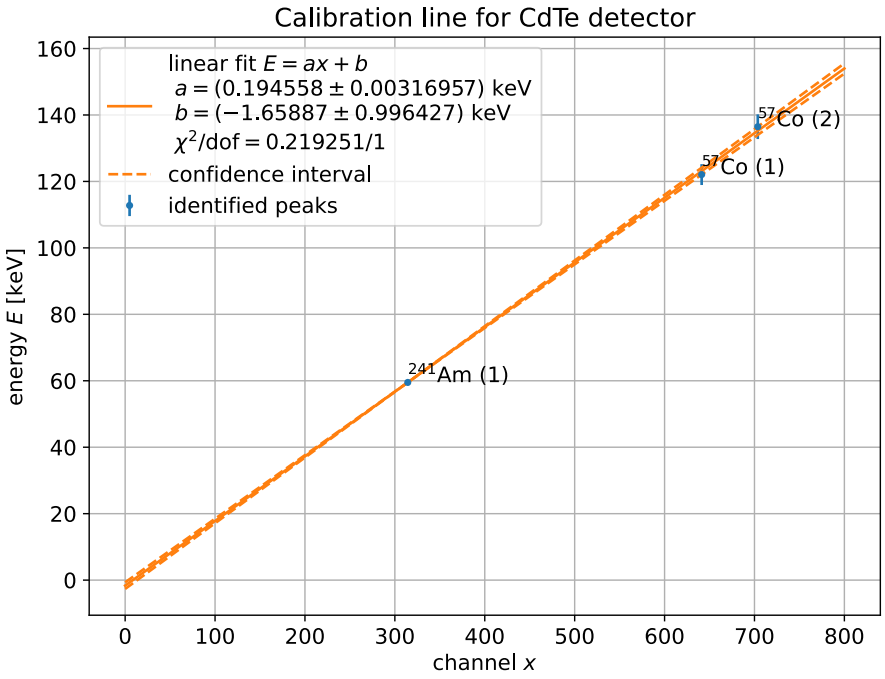

Figure 16: Energy calibration for the CdTe detector: linear fit to three known photopeaks.

$$s_{RER} = RER\,\frac{\Delta\sigma}{\sigma},$$

when using the given expected values of E for the three peaks and assuming their uncertainty to be negligible.

This gives us the following relative energy resolutions:

$$RER_{\mathrm{Si}}(59.9\,\mathrm{keV}) \approx 2(1) \tag{22}$$
$$RER_{\mathrm{Ge}}(59.9\,\mathrm{keV}) \approx 0.085(1) \tag{23}$$
$$RER_{\mathrm{Si}}(122.06\,\mathrm{keV}) \approx 0.5(3) \tag{24}$$
$$RER_{\mathrm{Ge}}(122.06\,\mathrm{keV}) \approx 0.097(19) \tag{25}$$
$$RER_{\mathrm{Si}}(136.47\,\mathrm{keV}) \approx 2(2) \tag{26}$$
$$RER_{\mathrm{Ge}}(136.47\,\mathrm{keV}) \approx 0.017(18) \tag{27}$$

5 Discussion

5.1 Discussion Part 1: Energy Bandgap E_g

We compare the obtained results for the bandgap energies $E_{\mathrm{g,Si}}$ (eq. (2)) and $E_{\mathrm{g,Ge}}$ (eq. (3)) for silicon and germanium with the reference values given in the instructions [Fre]:

$$E_{\mathrm{ref,Si}} = 1.12\,\mathrm{eV} \tag{28}$$
$$E_{\mathrm{ref,Ge}} = 0.66\,\mathrm{eV} \tag{29}$$

The relative deviations are

$$s_{\text{rel,Si}} = \frac{E_{\text{ref,Si}} - E_{\text{g, Si}}}{E_{\text{ref,Si}}} \approx 4\%$$
$$s_{\text{rel,Ge}} = \frac{E_{\text{ref,Ge}} - E_{\text{g, Ge}}}{E_{\text{ref,Ge}}} \approx 15\%.$$

Or in terms of standard deviations of the calculated quantities:

$$t_{\text{Si}} = \frac{E_{\text{ref,Si}} - E_{\text{g, Si}}}{s_{\text{Si}}} \approx 0.1$$
$$t_{\text{Ge}} = \frac{E_{\text{ref,Ge}} - E_{\text{g, Ge}}}{s_{\text{Ge}}} \approx 0.25.$$

Both result are thus well acceptable within the frame of their experimental uncertainties. We note, however, that the determination of the bandgap energy of Silicon was much easier and also resulted in a relative uncertainty that is a almost a factor 4 better than the one for Germanium.
As mentioned before, the transmission spectrum of Ge looked much more noisy and uneven when compared with the one of Si. This was also apparent during the data taking process through the fact that for Ge the highest possible gain (1000) on the pyro channel had to be chosen, while it was enough to use a much smaller gain setting (10) for the Si probe. This can be explained by different factors. We have used different filters for the two measurement series and the one used with the germanium sample was much less transparent as we could see comparing the lamp spectra. Lower intensity of the incoming light means that noise has a larger impact. Moreover, one can take into account that Si has a much larger bandgap (around factor 2) than Ge. The smaller bandgap in Ge leads to absorption in a broad range of the radiation spectrum, which in its turn increases the probability for noise to occur. The small bandgap possibly also allows for more thermal creation of charge carriers at room temperature. Si, on the other hand, is transparent for much larger parts of the spectrum. Other differences between the two materials might include factors like the amount of impurities or defects, which might also be responsible for heightened background radiation and noise.
Another factor which might have reduced the quality of the experiment conducted is the fact that the data acquisition software did not reliably keep the 0° position, which therefore had to be adjusted manually a few times in between different spectra (lamp, background,...) could be taken. The accuracy with which the 0° position can be found by hand is limited, but had this only been necessary once at the beginning of the experiment, then the here caused systematic error would have been equalised completely by taking the average of the left and the right spectrum. As it was, however, several small shifts between the different measurements taken with the same probe might have occurred, leading to a reduced accuracy of the overall dataset.

5.2 Discussion Part 2: Semiconductor Detector

In this part of the experiment, three peaks from the ^{57}Co and ^{241}Am spectrum were fitted and the parameters resulting from the fits were used in order to characterise the two different detectors in terms of their relative absorption probabilities and their relative energy resolutions.

The experimental results for the relative absorption probabilities, as given in eq. (18), indicate that the absorption probability of the Si diode detector system is a factor 2-30 higher than the absorption probability of the CdTe crystal detector. This result does not necessarily meet our expectations. As Cd and Te have higher atomic numbers than Si, one might assume that the probability for photons to interact with the detector material and loose energy to it should be higher and that the CdTe detector should thus have a higher absorption probability.

The relative energy resolutions obtained in the experiment, given in eq. (22), can be summarised by saying that they appear to be much better for CdTe (values < 0.1) than for Si (values > 0.5). This does not really meet our expectations either. As Si has a rather wide bandgap, the intrinsic energy resolution would be expected to be quite good and it would furthermore seem logical that a diode operated in reverse bias mode should do a better job at creating clean signals than an ohmic contact which has no intrinsic direction of free carrier flow.

We thought of several factors which might have contributed to us obtaining results in this experiment which differ so strongly from our expectation. One major source of uncertainty and potential

experimental inaccuracy is the fact that it was quite hard in both the ^{57}Co spectra obtained with either of the detectors to discern the second, smaller expected photopeak. It might have been possible that instead of the actual peak, which was covered deeply in noise, some unrelated component of the background was fitted. As the result of this fit had a big impact on the energy calibration, which in its turn had a big effect on how the parameters A and σ in energy units were calculated, a wrongly chosen fitting interval for the smaller ^{57}Co might have had a substantial effect. It might have been easier to fit this peak if a background spectrum had been taken and subtracted, for instance.

A second idea is that potentially something might have changed in the whole experimental setup during the weekend (between the Si detector measurement and the ones with the CdTe crystal) or during the changing of the detector components. This could be everything from a part of the electronics being influenced to the data acquisition software having had an update. This is however all very speculative and difficult to get a handle on, as there are so many different detector components.

Finally, it might be a possibility that the electronics (amplifier, MCA, ...) were in fact better optimised to work in combination with one of the two detector types. It should also be kept in mind that properties like the relative energy absorption of a detector are strongly dependant of factors like the quality of the detector material, its thickness, the ambient temperature or the used electronics.

6 Improvements and Suggestions

There are a few factors which limited the accuracy with which data could be taken in the experiment conducted by us and the following paragraph mentions some of these factors as well as offering some suggestions for how the procedure could have been improved.

For the first part of the experiment during which the bandgap energy E_{g} of Si and Ge should be determined, we struggled to really optimise the light path and noted how the beam was not in fact falling fully onto the sample. Even though the lenses and blind could be translated along the arms of the spectrometer, there was no possibility of for example tilting them. By using optical components with more possibilities for adjustments, one might have been able to better focus the light beam onto the grating and towards the sample as well as achieve a more parallel beam. A parallel beam is not only desirable from a loss of intensity point of view, but the width of the beam also plays a crucial role in the energy resolution of the spectrometer.

For both parts of the experiment, the data acquisition software used did unfortunately not work without faults. For the bandgap experiment, it was an unnecessary source of error that the program kept loosing the zero-point of the angle recording and for the detector experiment, long measurement sets were lost due to the program crashing unexpectedly. Using updated versions of the programs or more reliably working alternatives might make the data taking process easier and less error-prone.

Due to the limited lab hours in the advanced laboratory, the data acquisition time for the ^{241}Co spectra was chosen to be 3 h, after which the quality of the obtained spectrum still was not as good as for ^{241}Am. Better result might have been obtained by choosing even longer times. On a similar note, it might have been interesting to take an underground spectrum (for example over night) in order to be able to compare this with or subtract it from the spectra of the used isotopes.

Instead of choosing longer data acquisition times, it is also worth to consider using different radioactive sources, as the working of the detector and not the characteristics of the recorded gamma spectra were the focus of this experiment. Cleaner spectra might possibly been obtained within less time by using collimated and highly active sources like ^{137}Cs.

7 Conclusion

This series of experiments was dedicated to gaining some insight into the characteristic qualities of semiconductors and their usage in detector systems. In the first experiment, the bandgap energies E_g of Silicon and Germanium were determined using a spectrometer and the end results were compared with literature reference values. For Silicon this yields:

$$\begin{aligned} E_{g,Si} &= 1.07(42)\,\text{eV} \\ E_{ref,Si} &= 1.12\,\text{eV} \\ s_{rel,Si} &\approx 4\% \\ t_{Si} &\approx 0.1 \end{aligned}$$

And for Germanium:

$$\begin{aligned} E_{g,Ge} &= 0.56(38)\,\text{eV} \\ E_{ref,Ge} &= 0.66\,\text{eV} \\ s_{rel,Ge} &\approx 15\% \\ t_{Ge} &\approx 0.25 \end{aligned}$$

It was noted that the spectra of Ge were much lower in intensity and contained more noise in comparison to the Si spectra and some reasons for this were briefly discussed.

In the second part of the experiment, two different detector systems, one Si diode and one CdTe crystal with an ohmic contact with gold, were used to record and analyse the gamma spectra of ^{57}Co and ^{241}Am.
Three known photopeaks were fitted with Gaussian functions and the maximum positions of the fitted Gaussian curves were used to perform energy calibrations for both of the detectors. The fit parameters A and σ were used to calculate the relative absorption probabilities Abs_{Si}/Abs_{CdTe} for the three peaks, as well as the relative energy resolutions RER at the respective energies. These functions were used as a measure for comparing the two different detector types.
The experimental results indicate that the absorption probabilities of the Si detector are on average higher that the absorption probabilities for the CdTe detector and that the CdTe detector features comparatively higher relative energy resolutions. Both of these results appear opposite to what we would have expected, as explained in more detail in the discussion. Some ideas for why this discrepancy might have arisen are discussed as well.

Finally, a few ideas for how the experimental procedure could have been improved have been considered.

References

[Amr08] Simon Amrein. *Halbleiter und Halbleiterdetektoren.* Staatsexamensarbeit. 2008. URL: https://ilias.uni-freiburg.de/goto.php?target=file_3498665_download&client_id=unifreiburg

[Fre] Universität Freiburg. *Versuchsanleitung Fortgeschrittenen Praktikum Teil 1 Halbleiter.* URL: https://ilias.uni-freiburg.de/goto.php?target=file_3498664_download&client_id=unifreiburg

8 Appendix A: Calculation for energy calibration

We need to know how to convert the fit results for the peak parameters A and σ into $\tilde{A}$ and $\tilde{\sigma}$ using the energy calibration relation $E(X_\mathrm{c}) = a \cdot x_\mathrm{c}$. For this, we make the following considerations:

We want the total Gaussian peak descriptions to be the same:

$$c(x) = A \cdot \frac{1}{\sqrt{2\,\pi\sigma}} \cdot \exp\left(\frac{(x - x_\mathrm{c})^2}{2\,\sigma^2}\right) \stackrel{!}{=} \tilde{A} \cdot \frac{1}{\sqrt{2\,\pi\sigma}} \cdot \exp\left(\frac{(E - E_\mathrm{c})^2}{2\,\tilde{\sigma}^2}\right)$$

As we want the total amplitude of the peaks to be the same, also the exponential functions need to be the same and we can write:

$$\frac{x - x_\mathrm{c}}{\sigma} = \frac{E - E_\mathrm{c}}{\tilde{\sigma}} = \frac{a \cdot (x - x_\mathrm{c})}{\tilde{\sigma}}$$

and get

$$\begin{aligned} \tilde{\sigma} &= a \cdot \sigma \\ \Delta\tilde{\sigma} &= \sqrt{(a\,\Delta\sigma)^2 + (\sigma\,\Delta a)^2}. \end{aligned}$$

From the fact that the total amplitudes should be the same and using the above relationship, we take

$$A \cdot \frac{1}{\sqrt{2\,\pi\sigma}} \stackrel{!}{=} \tilde{A} \cdot \frac{1}{\sqrt{2\,\pi\tilde{\sigma}}},$$

and obtain

$$\begin{aligned} \tilde{A} &= A \cdot \frac{\tilde{\sigma}}{\sigma} = a \cdot A \\ \Delta\tilde{A} &= \sqrt{(a\,\Delta A)^2 + (A\,\Delta a)^2} \end{aligned}$$

9 Appendix B: Additional Plots

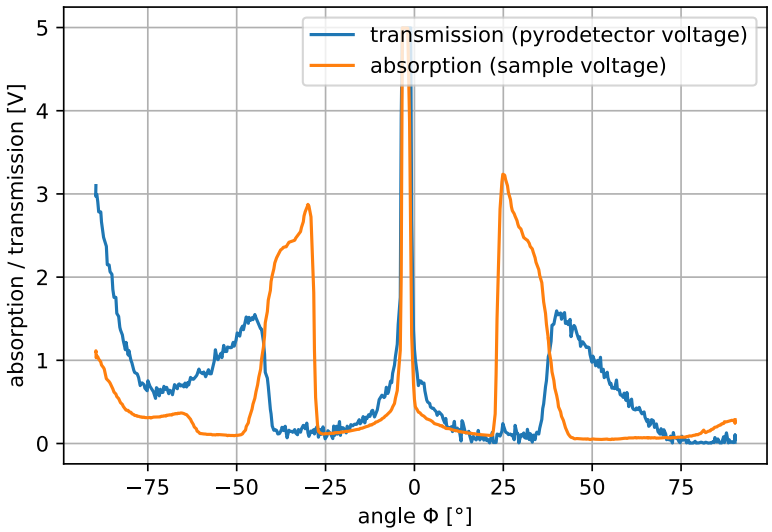

Figure 17: Data of the Si absorption and transmission spectrum as a function of the angle Φ before normalisation and background correction.

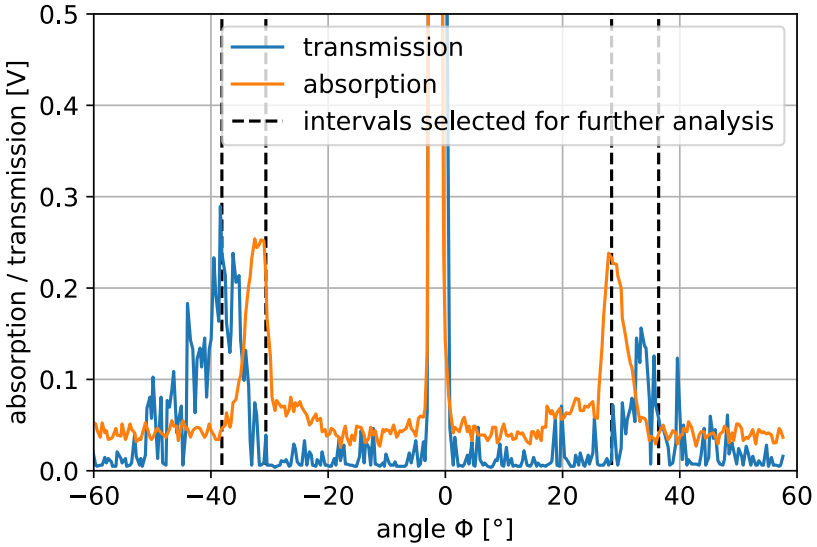

Figure 18: Data of the Ge absorption and transmission spectrum as a function of the angle Φ before normalisation and background correction.

10 Appendix C: Signed Lab Notes

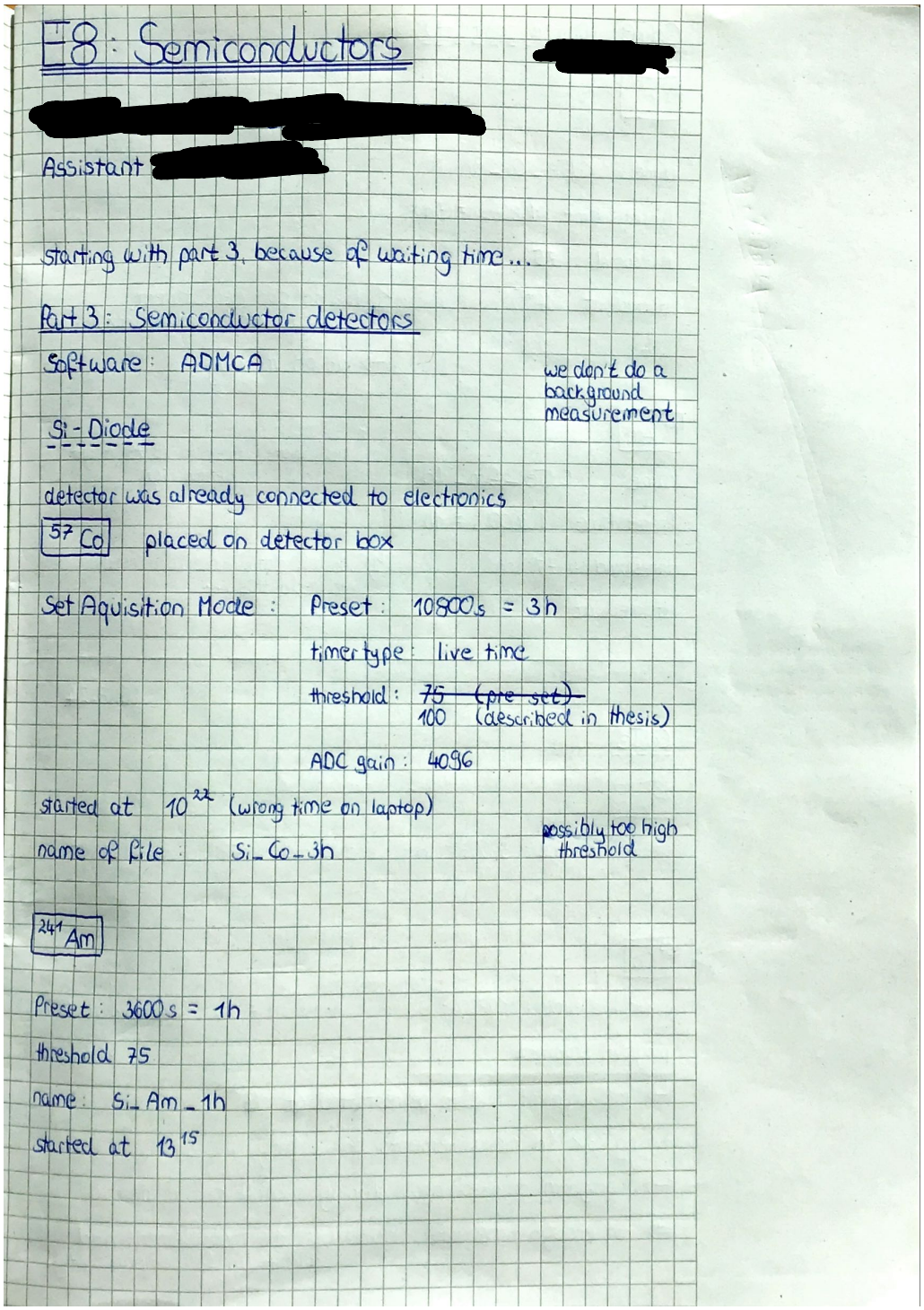

F8: Semiconductors

[redacted]

Assistant [redacted]

starting with part 3, because of waiting time...

Part 3: Semiconductor detectors

Software: ADMCA

we don't do a background measurement

Si-Diode

detector was already connected to electronics

^{57}Co placed on detector box

Set Aquisition Mode: Preset: 10800s = 3h

timer type: live time

threshold: ~~75 (pre-set)~~ 100 (described in thesis)

ADC gain: 4096

started at 10^{22} (wrong time on laptop)

name of file: Si_Co_3h

possibly too high threshold

^{241}Am

Preset: 3600s = 1h

threshold 75

name: Si_Am_1h

started at 13^{15}

Figure 19: Lab notes page 1

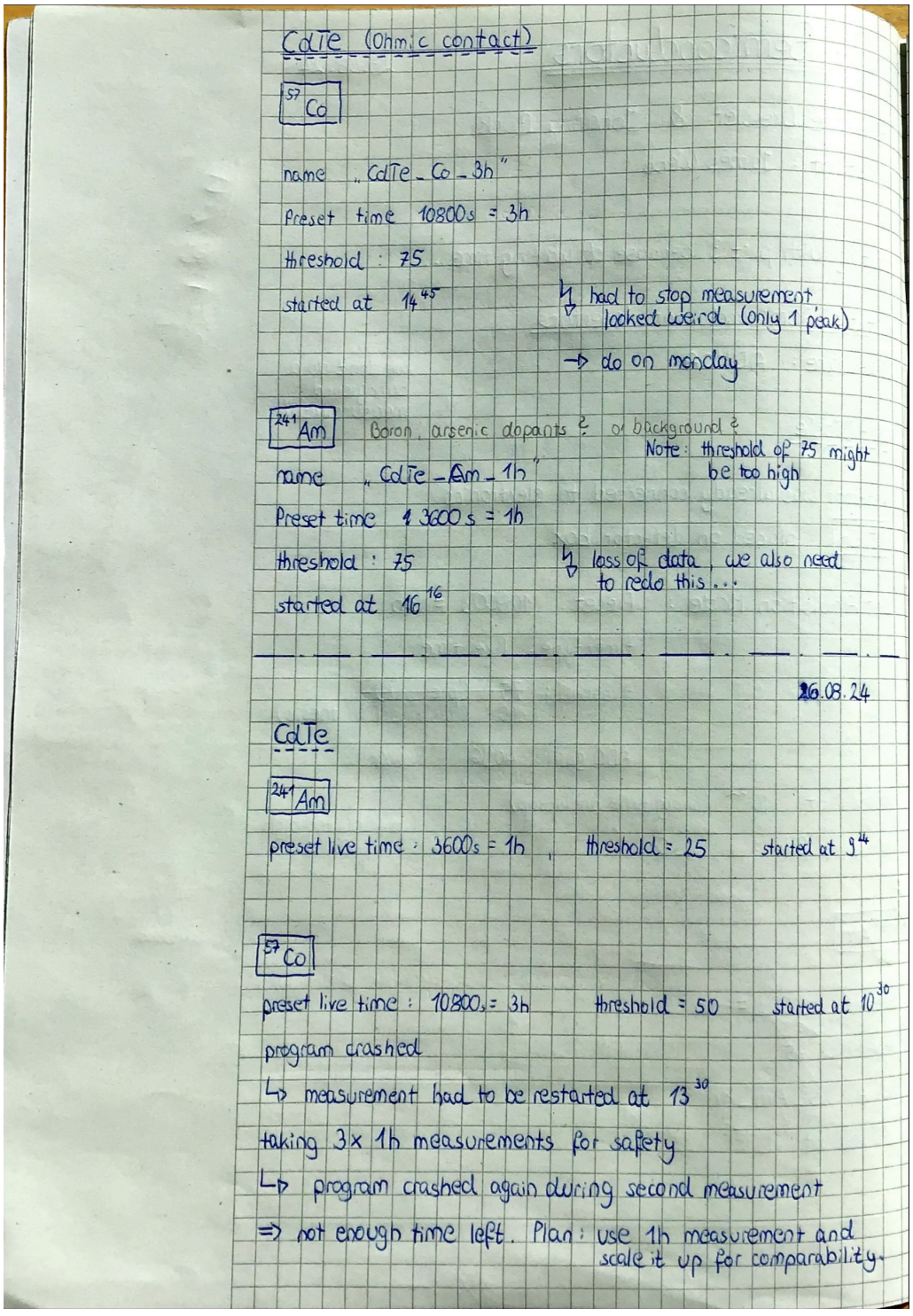
CdTe (Ohmic contact)

^{57}Co

name „CdTe_Co_3h"

Preset time 10800s = 3h

threshold: 75

started at 14^{45}

↳ had to stop measurement, looked weird (only 1 peak)

→ do on monday

^{241}Am Boron, arsenic dopants ? or background ?

Note: threshold of 75 might be too high

name „CdTe_Am_1h"

Preset time 3600s = 1h

threshold: 75

started at 16^{16}

↳ loss of data, we also need to redo this...

26.08.24

CdTe

^{241}Am

preset live time: 3600s = 1h, threshold = 25 started at 9^{44}

^{57}Co

preset live time: 10800s = 3h threshold = 50 started at 10^{30}

program crashed

↳ measurement had to be restarted at 13^{30}

taking 3x 1h measurements for safety

↳ program crashed again during second measurement

⇒ not enough time left. Plan: use 1h measurement and scale it up for comparability.

Figure 20: Lab notes page 2

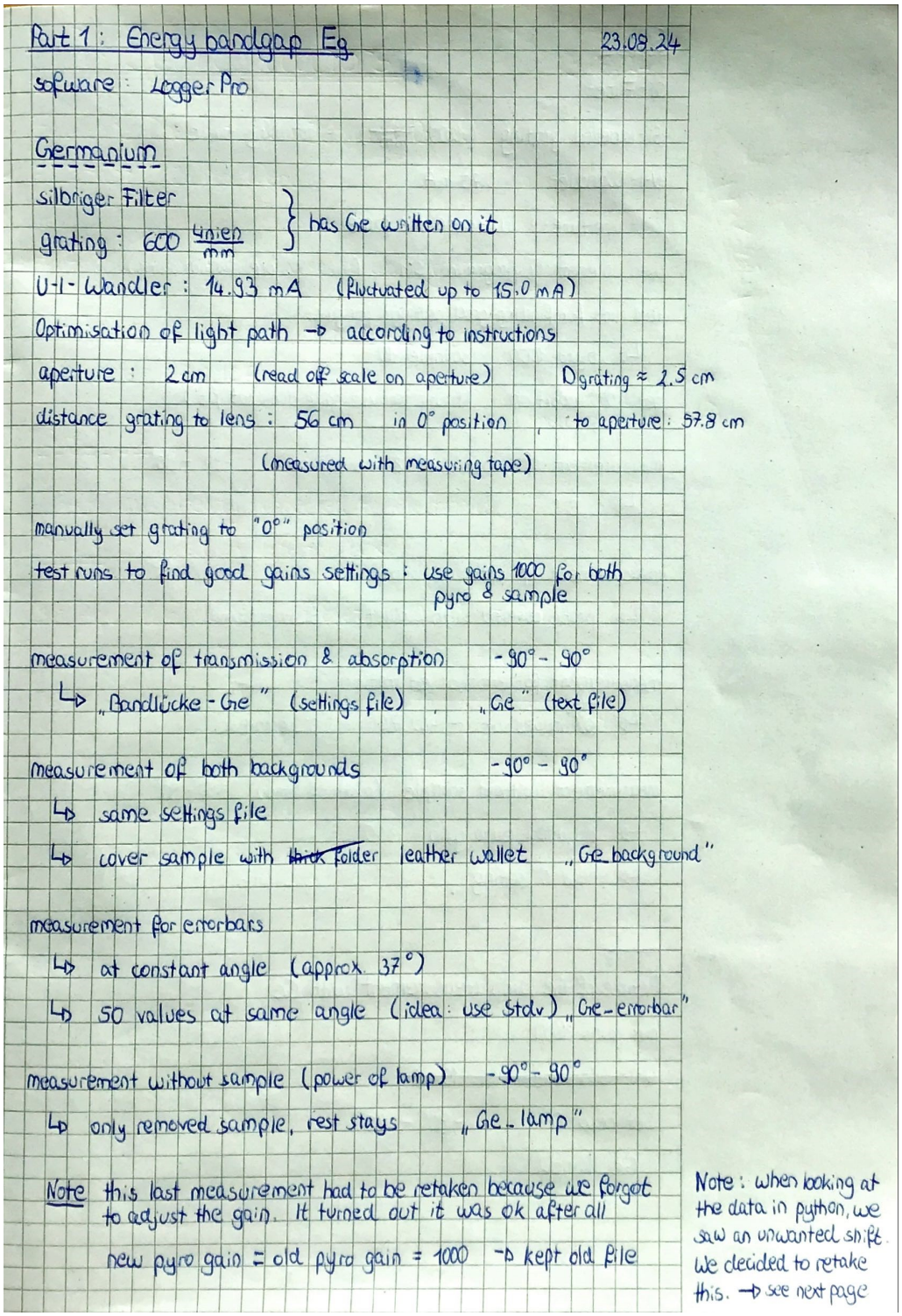
Part 1: Energy bandgap Eg 23.08.24

software: Logger Pro

Germanium

silbriger Filter
grating: 600 Linien/mm
} has Ge written on it

U-I-Wandler: 14.93 mA (fluctuated up to 15.0 mA)

Optimisation of light path → according to instructions

aperture: 2 cm (read off scale on aperture) D grating ≈ 2.5 cm

distance grating to lens: 56 cm in 0° position, to aperture: 57.8 cm
(measured with measuring tape)

manually set grating to "0°" position

test runs to find good gains settings: use gains 1000 for both pyro & sample

measurement of transmission & absorption -90° - 90°
↳ „Bandlücke-Ge" (settings file), „Ge" (text file)

measurement of both backgrounds -90° - 90°
↳ same settings file
↳ cover sample with ~~thick~~ folder leather wallet „Ge_background"

measurement for errorbars
↳ at constant angle (approx. 37°)
↳ 50 values at same angle (idea: use Stdv) „Ge-errorbar"

measurement without sample (power of lamp) -90° - 90°
↳ only removed sample, rest stays „Ge_lamp"

Note this last measurement had to be retaken because we forgot to adjust the gain. It turned out it was ok after all
new pyro gain = old pyro gain = 1000 → kept old file

Note: when looking at the data in python, we saw an unwanted shift. We decided to retake this. → see next page

Figure 21: Lab notes page 3

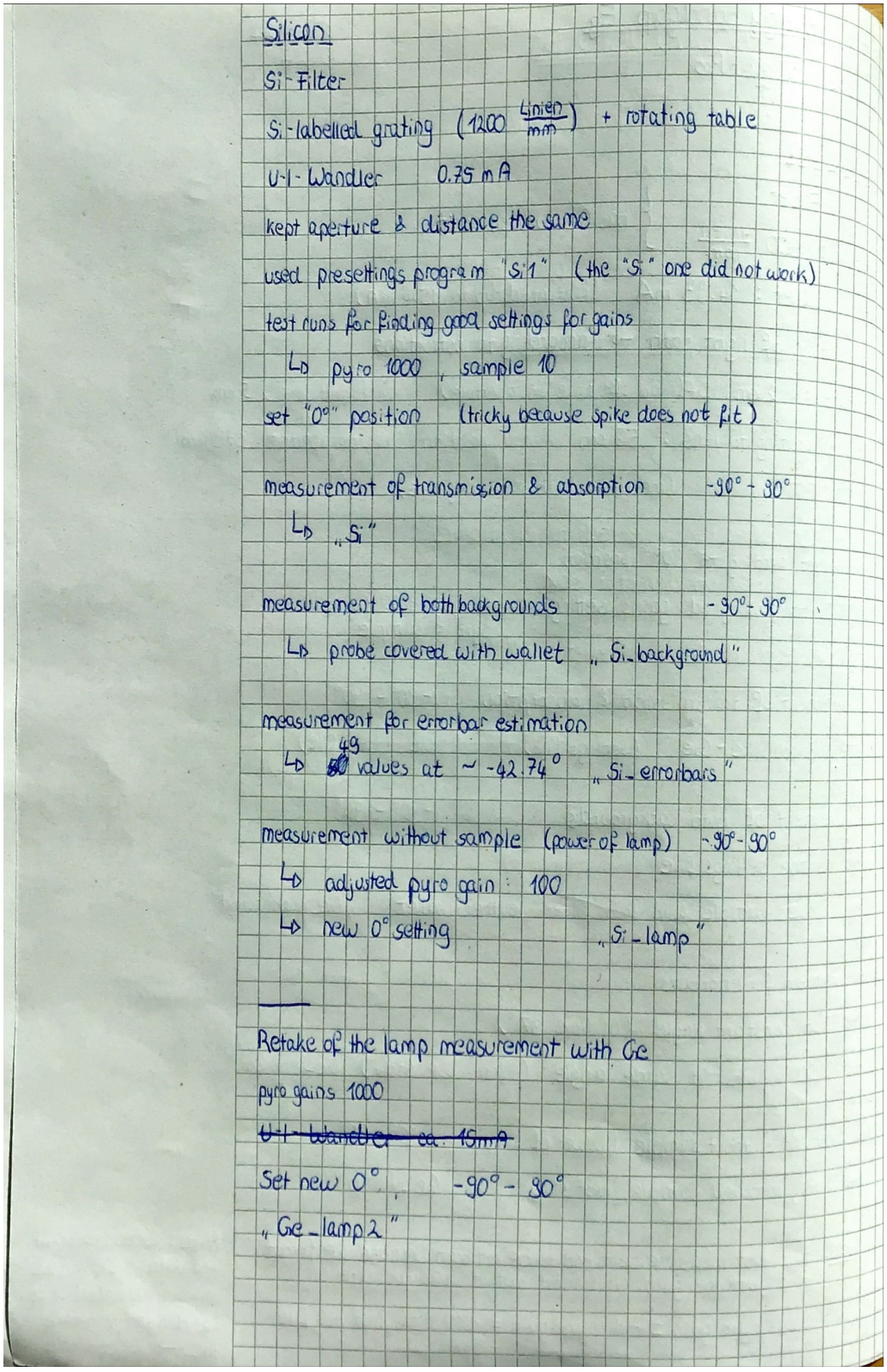

Figure 22: Lab notes page 4

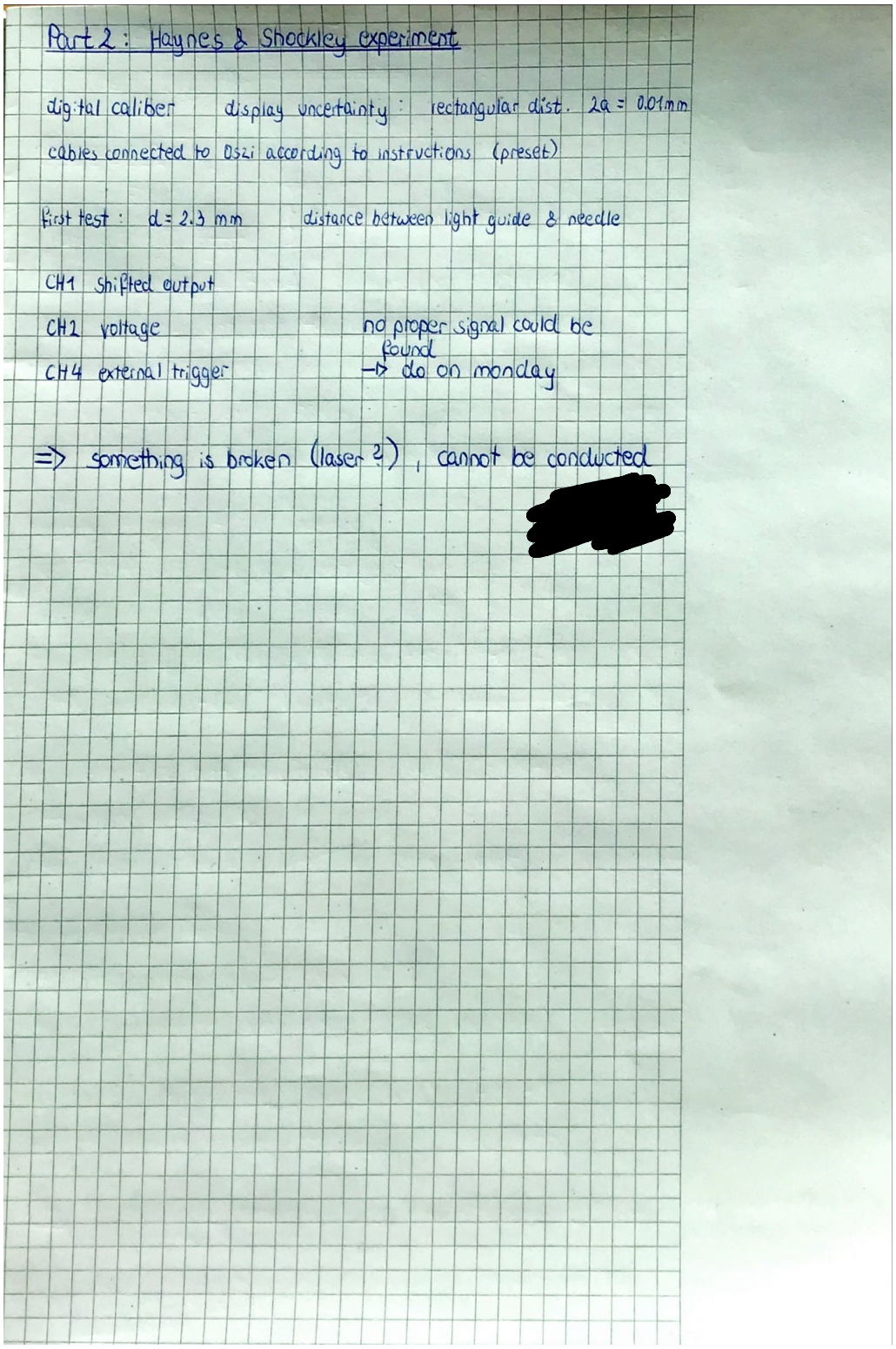

Figure 23: Lab notes page 5